International Conference on Applied Energy 2020
Dec. 1 - Dec. 10, 2020, Bangkok / Virtual
Paper ID: 130

Multi-stage Charging Strategy of Lithium-ion Battery Considering Aging Effect and Energy Loss

Jiaqiang Tian, Ruilong Xu, Zonghai Chen*

Department of Automation, University of Science and Technology of China, Hefei, Anhui 230027, PR China

ABSTRACT

In order to reduce battery aging and energy loss, an optimized charging method considering battery aging and energy loss is proposed in this work. Firstly, based on the second-order RC equivalent circuit model, the parameters of the battery model are identified by pulse current tests. Secondly, according to Joule's law, the model of battery energy loss is established. Combining the established model with the aging empirical model, the dual objective of charging optimization is constructed. The non-terminated sorted genetic II algorithm is used to optimize goals. The utopian point method is applied to select the best target and determine the optimal charging current sequence. Finally, the effectiveness of the proposed method is verified by comparative experiments. The experimental results show that the overall effect of 8-stage current charging is better than that of 4-stage charging, which has better benefits for improving battery performance.

Keywords: Aging empirical model, Charging optimization, Non-terminated sorted genetic II algorithm, Utopian point method

1. INTRODUCTION

As a clean and environment-friendly energy storage device, the lithium-ion battery has the advantages of high energy density, low self-discharge rate, and long service life [1]. It is widely used in electric vehicles, microgrid, aerospace [2]. The lithium-ion battery has life decay characteristics, and its aging is affected by operating conditions and charging modes. Since the former depends on the load, which is uncontrollable. Therefore, to alleviate the battery aging, a reasonable charging mode is required.

Many scholars have proposed a variety of effective charging strategies. According to its principle, they can be summarized as the following categories: (a) Constant current and constant voltage (CC-CV) charging. Its principle is as follows: firstly, the battery is charged to the cut-off voltage with the constant current, then it is charged in the mode of constant-voltage. When the current decays to the cut-off current, the charging is completed. In the constant voltage charging stage, the small current can alleviate battery aging, but it will consume more time [3]. (b) Multi stage constant current charging. For this strategy, the constant voltage stage is replaced by a group of gradually decreasing current. When the battery voltage rises to the maximum value, the charging current is changed to a smaller current. In Ref. [4], an adaptive multi-stage constant current charging strategy is proposed based on the thermoelectric coupling model and particle swarm optimization algorithm. The experimental results show that the charging time is 37% shorter than the traditional charging method. (c) Pulse charging. The principle of this method is as follows: firstly, the battery is charged at the preset current for a period of time, then the battery is rested or discharged by short-term negative pulse. In Ref. [5], by adjusting the pulse frequency and duty cycle to reduce the battery polarization, the maximum capacity is charged in less than 20 minutes, which is two times faster than the traditional CC-CV charging method. (d) Boost charging. In the initial stage of charging, the battery is charged to the cut-off voltage or predetermined time at a high current rate. Then the traditional CC-CV charging method is executed. The purpose is verified in Ref. [6]. The research shows that compared with the conventional CC-CV charging method, the charging speed is significantly faster without any negative impact on the cycle life of the battery. (e) Constant polarization voltage charging. Based on the relationship between polarization voltage, SOC, and current, the charging current is optimized to minimize the polarization effect. According to the polarization

*Corresponding author. Z. Chen. E-mail address: chenzh@ustc.edu.cn.
Selection and peer-review under responsibility of the scientific committee of the 12th Int. Conf. on Applied Energy (ICAE2020).

time constant, the acceptable charging current curve is established in Ref. [7]. The charging current under different SOC can be calculated with the constraints of polarization voltage and cut-off voltage. The experimental results show that the battery can be charged from 20% to 80% of SOC in 33 minutes, and its average polarizability and maximum temperature rise are similar to CC-CV charging at 0.5C.

The methods mentioned above rarely optimize the charging strategy aiming at the aging effect, so the strategy may not be optimal for delaying aging. Besides, most approaches do not consider the loss of charging energy. To address the above issues, this paper proposes a charging strategy optimization method considering the aging effect and energy loss.

2. SYSTEM MODELING

2.1 Energy loss model

As one of the commonly used equivalent circuit models (ECMs) of lithium-ion batteries, the second-order RC ECM has high accuracy, which can accurately describe the voltage characteristics of lithium-ion batteries [8]. The structure of second-order RC ECM is shown in Fig. 1(a). Its state equation can be described as Eq. (1).

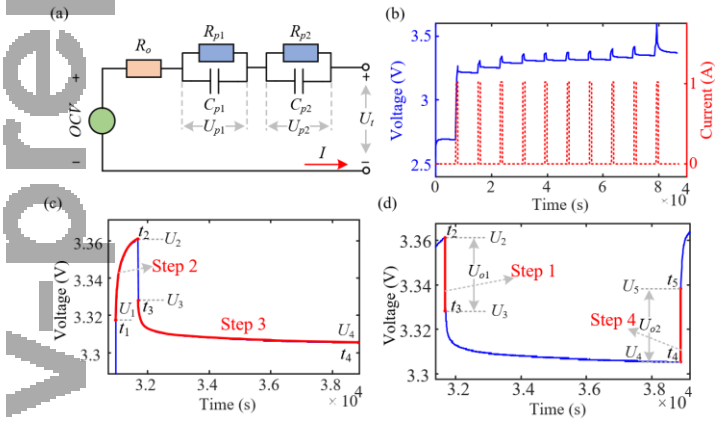

Fig. 1 Battery model and OCV test. (a) Second-order RC ECM. (b) OCV test conditions. (c) Ohmic response. (d) polarization response.

$$\begin{cases} U_{p1,k} = e^{-\Delta t/(R_{p1,k}C_{p1,k})}U_{p1,k-1} + \left(1-e^{-\Delta t/(R_{p1,k}C_{p1,k})}\right)R_{p1,k}I_k \\ U_{p2,k} = e^{-\Delta t/(R_{p2,k}C_{p2,k})}U_{p2,k-1} + \left(1-e^{-\Delta t/(R_{p2,k}C_{p2,k})}\right)R_{p2,k}I_k \\ OCV_k = k_0 + k_1 \cdot SOC_k + k_2 / SOC_k + k_3 \cdot (SOC_k)^2 + k_4 \cdot \ln(SOC_k) + k_5 \cdot \ln(1-SOC_k) \\ U_{t,k} = OCV_k + U_{p1,k} + U_{p2,k} + R_{o,k}I_k \end{cases} \quad (1)$$

Where $U_{pi,k}$, $C_{pi,k}$ and $R_{pi,k}$ (i=1,2) represent the polarization voltage, polarization capacitance, and polarization resistance of the ith RC network, respectively. $R_{o,k}$ and I_k denote the ohmic resistance and current, respectively. OCV_k and $U_{t,k}$ represent the open-circuit voltage (OCV) and terminal voltage, respectively. Δt represents the sampling time. k_i (i=0,1,…,5) denotes the coefficients of OCV function. The definition of SOC is shown in Fig. (2).

$$SOC_k = SOC_{k-1} + \Delta t \cdot I_k \cdot \eta / Q_0 \quad (2)$$

where η and Q_0 denote the coulomb efficiency and capacity of the battery, respectively.

To obtain the model parameters, the impulse excitation method is applied. The test conditions are shown in Fig. 1(b). The specific working conditions are as follows: firstly, the battery is discharged to the cut-off voltage (2V) with constant current, and then it is rested for 2h. At this time, the voltage is taken as the OCV when SOC=0. Then the battery is charged with $0.1Q_0$ under the constant current, and rest it for 2h. After 10 cycles, OCV under different SOC points can be obtained. Fig. 1(d) shows the ohmic voltage response curve, as Step 1. Therefore, the ohmic voltage drop can be expressed as:

$$U_{o1} = U_2 - U_3 \quad (3)$$

Similarly, U_{o2} is the ohmic voltage drop caused by the imposed current. So, the ohmic resistance can be obtained from the following formula:

$$R_o = \frac{U_{o1}+U_{o2}}{2 \cdot \Delta I} = \frac{(U_2-U_3)+(U_5-U_4)}{2 \cdot \Delta I} \quad (4)$$

In Fig. 1(c), Step 2 is composed of OCV and RC network zero state response. The zero state responses of RC networks can be expressed as follows (i=1,2):

$$U_{p,i}(t) = R_{p,i} \cdot I \cdot (1-e^{-t/(R_{p,i}C_{p,i})}) \quad (5)$$

For Step 3, it is caused by zero input responses of RC networks, which can be expressed as follows:

$$\begin{aligned} U_p(t) &= U_3(t_3) - U_4(t) \\ &= U_{p1}(t_2)e^{-t/(R_{p1}C_{p1})} + U_{p2}(t_2)e^{-t/(R_{p2}C_{p2})} \end{aligned} \quad (6)$$

Based on the above analysis, the time constant and polarization voltage at t_2 can be identified by the least square fitting. Subsequently, the polarization resistance can be calculated as Eq. (7).

$$R_{p,i} = \frac{U_{p,i}(t_2)}{I \cdot (1-e^{-(t_2-t_1)/(R_{p,i}C_{p,i})})} \quad (7)$$

According to Joule's law, the ohmic resistance and polarization resistance will consume energy during charging and discharging, which can be described as:

$$E_{loss} = \sum_{k=0}^{k=N} \left(R_{o,k}{I_k}^2 + R_{p1,k}{I_{p1,k}}^2 + R_{p2,k}{I_{p2,k}}^2\right)\Delta t \quad (8)$$

where E_{loss} denotes the loss of energy. $I_{p1,k}$ and $I_{p2,k}$ denote the polarization current of two RC networks. Considering that ohmic resistance and polarization resistance are sensitive to SOC, Eq. (8) is modified as:

$$E_{loss}=\sum_{k=0}^{k=N}\left(R_{o,k}(\mathrm{SOC}_k)I_k^{\,2}+R_{p1,k}(\mathrm{SOC}_k)I_{p1,k}^{\,2}+R_{p2,k}(\mathrm{SOC}_k)I_{p2,k}^{\,2}\right)\Delta t \quad (9)$$

2.2 Capacity loss model

In the usage of lithium-ion batteries, we focus on the cycle aging rather than calendar aging. A large number of literature has carried out in-depth research on lithium-ion cycle aging. In Ref. [9], a series of aging experiments are carried out on A123 LiFePO4 battery (ANR26650M1-A), and the aging empirical model with the current ratio is constructed, as shown in Eq. (10).

$$Q_{loss}=A(c)\cdot e^{-\frac{E_a(c)}{RT}}A_h(c)^z \quad (10)$$

where Q_{loss} denotes the normalized capacity loss, which is defined as Eq. (6). $A(\cdot)$, $E_a(\cdot)$ and $A_h(\cdot)$ represent the pre-exponential factor, activation energy, and ampere-hour throughput, which are functions of the current rate, as Eqs. (12)-(14). R, T and z denote the ideal gas constant, temperature, and law factor [10].

$$Q_{loss}=\frac{Q_{int}-Q_{cur}}{Q_{int}}\times 100\% \quad (11)$$

where Q_{int} and Q_{cur} represents the initial capacity and the current capacity, respectively.

$$A(c)=-47.836c^3+1215c^2-9418.9c+36042 \quad (12)$$

$$E_a(c)=31700-370.3c \quad (13)$$

$$A_h(c)=A_{h0}+\frac{1}{3600}\int|c\cdot Q_0|dt \quad (14)$$

3. CHARGING STRATEGY BASED ON DOUBLE OBJECTIVE OPTIMIZATION

In order to optimize the charging current, a multi-stage constant current charging strategy is adopted. Ref. [11] shows that the ohmic resistance and polarization resistance in the low-end SOC region is significant, the battery energy consumption in this region is serious. The ohmic resistance is small and stable in the middle SOC region, and the battery has better performance in this range. The maximum usable capacity of high-end SOC battery declines rapidly, and the thermal performance declines severely in this region. Therefore, the charging current is optimized in the middle of SOC (10% ~ 90%). Since the charging current of multi-stage constant current charging is constant in each charging stage, the energy loss of charging can be regarded as the sum of several single-stage charging energy losses. Capacity loss is also the cumulative effect of multiple charging stages. Then, the dual objective of charging optimization can be defined as:

$$\begin{cases}\begin{cases}\min\ E_{loss}=\sum_{j=1}^{j=M+2}\left(R_{o,j}(\mathrm{SOC}_j)I_j^{\,2}+R_{p1,j}(\mathrm{SOC}_j)I_{p1,j}^{\,2}+R_{p2,j}(\mathrm{SOC}_j)I_{p2,j}^{\,2}\right)\frac{\Delta SOC_j\cdot Q_0}{\eta\cdot I_j}\\ \min\ Q_{loss,M+2}=Q_{loss,M+1}+\Delta A_{hM+2}zA\left(\frac{I_{M+2}}{Q_0}\right)e^{-\frac{E_a(I_{M+2}/Q_0)}{RT}}\left(\sum_{j=1}^{M+2}\Delta A_{hj}\right)^{z-1}\end{cases}\\ s.t\begin{cases}0\le \mathrm{SOC}\le 1\\ 2.0\mathrm{V}\le U_t\le 3.6\mathrm{V}\\ 0\le I_j\le 10c\end{cases}\end{cases} \quad (15)$$

where M represents the number of constant current charging stages, and ΔSOC represents the SOC variation in each charging stage. 0-10% SOC and 90% - 100% SOC are charged with specified current, which are not used as optimization interval. The non-terminated sorted genetic algorithm-II (NSGA-II) is one of the multi-objective genetic algorithms. It reduces the complexity of the non-inferior sorting genetic algorithm, and has the advantages of fast running speed and good convergence of solution set [12]. Therefore, in this study, it is used to optimize the charging current.

4. VALIDATION AND DISCUSSION

4.1 Parameter identification

In order to obtain the relationship between Ro, Rp, SOC, and current, the battery is tested by pulse current at the fixed SOC under 25 °C. The battery test system and thermostat are NEWARE CT-8004-5V200A-NTFA and SUYIDA GDW-100L, respectively. The testing condition is shown in Fig. 1(b). Currents are set to 0.5c, 1c, and 2c. Fig. 2(a) shows the fitting result of the zero input response curve of voltage. It can be seen from the figure that the measured value and the fitting value have a good coincidence degree, which means that the second-order RC equivalent circuit has good accuracy. According to Figs. 2(b)-(d), the ohmic resistance and polarization resistance are greatly affected by SOC, especially at the low SOC phase.

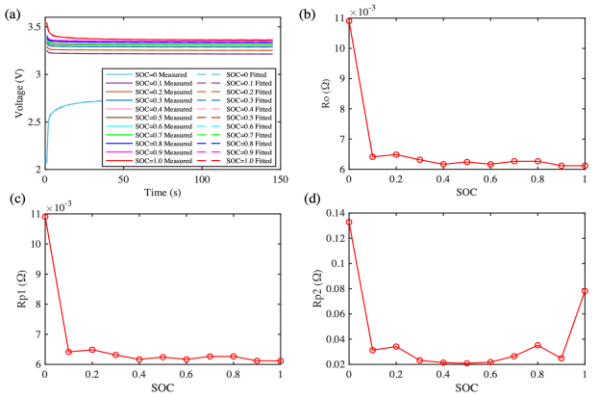

Fig. 2 Parameter identification results: (a) Voltage zero input response. (b) Ro. (c) Rp_1. (d) Rp_2.

4.2 Charging verification

It can be seen from Fig. 2 that the polarization resistance and ohmic resistance are large in the high and low SOC range. To reduce energy loss, 0.2c constant current charging is adopted when SOC < 0.1 and SOC > 0.9. Therefore, the SOC range of 0.1 ~ 0.9 is optimized in this work. In this paper, two comparative experiments are designed. Experiment 1: the current is optimized in 4 stages. Experiment 2: the current is optimized in 8 stages. Figs. 3(a) and (e) show the Pareto frontiers of optimization results.

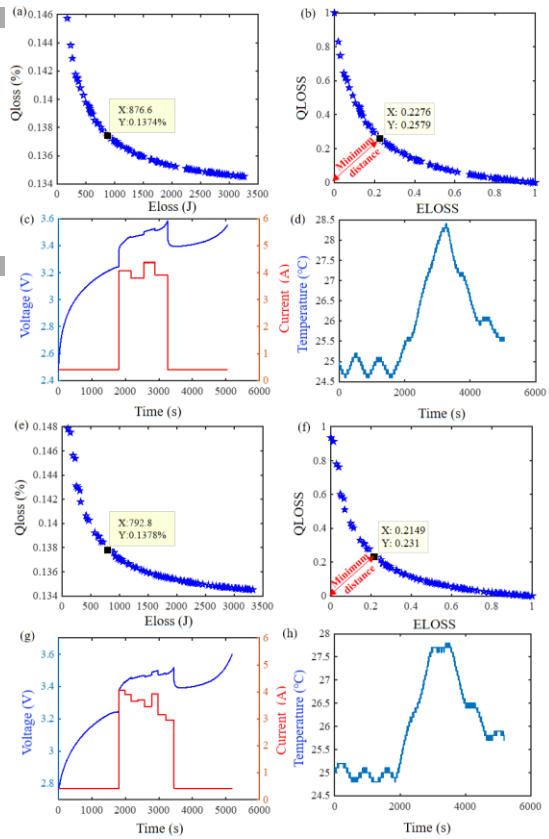

Fig. 3 Optimization results of charging: (a) Pareto frontier of Experiment 1. (b) Normalization of figure (a). (c) Current and voltage of Experiment 1. (d) Temperature of Experiment 1. (e) Pareto frontier of Experiment 1. (f) Normalization of figure (e). (g) Current and voltage of Experiment 2. (h) Temperature of Experiment 2.

It can be seen from the results that capacity loss and energy loss are contradictory. We use the utopian point method to select the final current condition. The point on the Pareto front which is the smallest distance from the utopian point is selected. To avoid the influence of target magnitude difference on the decision result, the original Pareto fronts are normalized, as shown in Figs. 3(b) and (f). The optimal decision point is determined by standardized Pareto frontier. For Experiment 1, the energy loss and capacity loss of the optimal point are 0.1374% and 876.6J, respectively. The optimized current is shown in Fig. 3(c). The battery reaches the charging cut-off voltage at 5057s, and the total charged capacity is 2.0337Ah. When the SOC is less than 0.1, the battery temperature remains relatively stable. When the SOC is in the range of 0.1-0.9, the temperature rise is obvious due to the large charging current. The maximum temperature is 28.2 °C. Similarly, the optimal capacity loss and capacity loss of Experiment 2 are 0.1378% and 792.8J, respectively. Compared with Experiment 1, energy loss is reduced by 9.56%. Capacity loss is increased by 0.2911%. In addition, the battery charging time is 5193s, the current is shown in Fig. 3(g). The optimized current is gradually decreasing, which can reduce the polarization effect of the battery at the end of charging, thus increasing the charging capacity. The total charging capacity of Experiment 2 is 2.0339Ah, which is similar to Experiment 1. The highest temperature of the battery is 27.6 °C, which is 2.13% lower than the former. In general, the optimization effect of Experiment 2 is better than that of Experiment 1. It shows that multi-stage optimization is more beneficial to reduce battery charge loss.

5. CONCLUSION

This paper proposes a charging optimization strategy considering capacity loss and energy loss. Based on the second order RC model and pulse current condition, the model parameters are identified. According to the Joule's law, the ohmic resistance and polarization resistance are the main components of energy loss. Further, the energy loss model is established. In addition, the aging empirical model is used as another optimization objective, and the NSGA-II is applied to optimize the current sequence. The results show that compared with 4-stage charging, the capacity loss of 8-stage charging is slightly increased, but the energy loss

and temperature rise are significantly reduced, and more power can be charged. It indicates that the reasonable charging can effectively improve the battery performance.

ACKNOWLEDGEMENT

This work is supported by the National Natural Science Fund of China (Grant No. 91848111).

REFERENCE

[1] Tian J, Wang Y, Liu C, et al. Consistency evaluation and cluster analysis for lithium-ion battery pack in electric vehicles[J]. Energy, 2020, 194: 116944.

[2] Wei Z, Zhao D, He H, et al. A noise-tolerant model parameterization method for lithium-ion battery management system[J]. Applied Energy, 2020, 268: 114932.

[3] Li Y, Li K, Xie Y, et al. Optimized charging of lithium-ion battery for electric vehicles: Adaptive multi-stage constant current–constant voltage charging strategy[J]. Renewable Energy, 2020, 146: 2688-2699.

[4] Chen L, Hsu R, Liu C. A Design of a Grey-Predicted Li-Ion Battery Charge System[J]. IEEE Transactions on Industrial Electronics, 2008, 55(10): 3692-3701.

[5] Yin M, Youn J, Park D, et al. Efficient Frequency and Duty Cycle Control Method for Fast Pulse-Charging of Distributed Battery Packs by Sharing Cell Status[C]. Ubiquitous intelligence and computing, 2015: 1813-1818.

[6] Notten P, Veld J, Beek J. Boost charging Li-ion batteries: A challenging new charging concept[J]. Journal of Power Sources, 2005, 145(1): 89-94.

[7] Jiang J, Liu Q, Zhang C, et al. Evaluation of acceptable charging current of power Li-ion batteries based on polarization characteristics[J]. IEEE Transactions on Industrial Electronics, 2014, 61(12): 6844-6851.

[8] Wang Y, Tian J, Sun Z, et al. A comprehensive review of battery modeling and state estimation approaches for advanced battery management systems[J]. Renewable and Sustainable Energy Reviews, 2020, 131: 110015.

[9] Wang J, Liu P, Hicks-Garner J, et al. Cycle-life model for graphite-LiFePO 4 cells[J]. Journal of Power Sources, 2011, 196(8): 3942-3948.

[10] Hu X, Johannesson L, Murgovski N, et al. Longevity-conscious dimensioning and power management of the hybrid energy storage system in a fuel cell hybrid electric bus[J]. Applied Energy, 2015, 137: 913-924.

[11] Lei Y, Zhang C, Gao Y, et al. Charging Optimization of Lithium-ion Batteries Based on Capacity Degradation Speed and Energy Loss[J]. Energy Procedia, 2018, 152:544-549.

[12] Liu D, Huang Q, Yang Y, et al. Bi-objective algorithm based on NSGA-II framework to optimize reservoirs operation[J]. Journal of Hydrology, 2020, 585: 124830.